

Quasimelting and Phases of Small Particles

P. M. Ajayan and L. D. Marks

Department of Materials Science, Northwestern University, Evanston, Illinois 60208

(Received 30 October 1987)

Calculations of the Gibbs free energies of single-crystal and multiply twinned small metal particles clearly indicate for the first time both the presence of a quasimolten phase (where the particles are continuously fluctuating between different structures) at temperatures well below the melting point and the existence of distinct phase regions for different particle shapes. These results have important implications for the understanding of epitaxial growth processes; for instance, at temperatures where the quasimolten and single-crystal phases are contiguous, one would expect far better epitaxial growth than at temperatures where the multiply twinned phases are stable.

PACS numbers: 61.50.Cj, 61.50.Jr, 68.55.Jk, 68.55.Rt

It has been known for many years that it is possible to produce small metal clusters which have different structures from the stable bulk solid structure, the most clear-cut example being multiply twinned particles.¹ The basic rationale for these structures is that they have lower total surface energy than simple single crystals because of more low-energy (111) faces at the expense of an internal strain; at smaller sizes the net gain in surface energy outweighs the strain-energy cost.² Some recent high-resolution electron microscope results³ have suggested that there may be some additional physics of interest in these particles. The experimental observation is that some small particles, rather than having a fixed structure, fluctuate between different multiply twinned and single-crystal structures on a time scale than can be observed by a real-time television image intensifier (i.e., remaining in each state for about $\frac{1}{30}$ sec). These results are suggestive of the structural fluctuations predicted by Hoare and Pal,⁴ who find that a very small cluster may have enough entropy not to remain in a fixed structure, and by Berry, Jellenik, and Natanson,⁵ who find a pseudomelting range in small particles.

Stimulated by these results, we have recently been working to extend previous continuum models² to consider more complicated particle structures, initially calculating part of the n -dimensional enthalpy surface as a function of the particle morphology.⁶ These calculations implied that the energy difference between different particle morphologies was surprisingly small, and we suggested that the fluctuations predicted by Hoare and Pal could be extended to much larger particle sizes, leading to the "quasimelting" observed in the electron microscope.

The intention of this Letter is to report the results of the extension of the model to include the entropy, which allows us to calculate part of the Gibbs-free-energy surface as a function of the particle morphology and the Boltzmann distribution of particle structures. We conclude from our analysis that there exists a true phase regime where quasimelting occurs, distinct from the con-

ventional melting of a small particle. In addition we construct for the first time a phase diagram for the thermodynamic equilibrium structures of small particles as a function of particle size and temperature.

The basic idea of the enthalpy calculation⁶ was to calculate the strain and total surface energies of asymmetric decahedral multiply twinned particles, one line along the n -dimensional surface. The largest contribution was the surface energy which was evaluated in terms of a dimensionless energy parameter

$$E_w = (\gamma_{111})^{-1} \int \gamma dS \left(\int dV \right)^{-2/3}, \quad (1)$$

which depends only on the particle shape (in this case the shape parameter b , which defines the geometric position of an asymmetric disclination from the particle

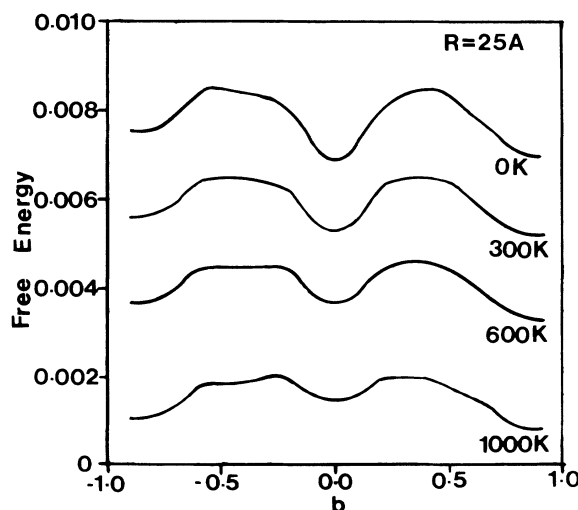


FIG. 1. Plots of the Gibbs free energy as a function of b , the fractional distance from the circular particle center of the disclination core in a decahedral multiply twinned particle, for different temperatures. The energy curves were plotted after normalization at each temperature individually and compression of scale on the Y axis for better visual display.

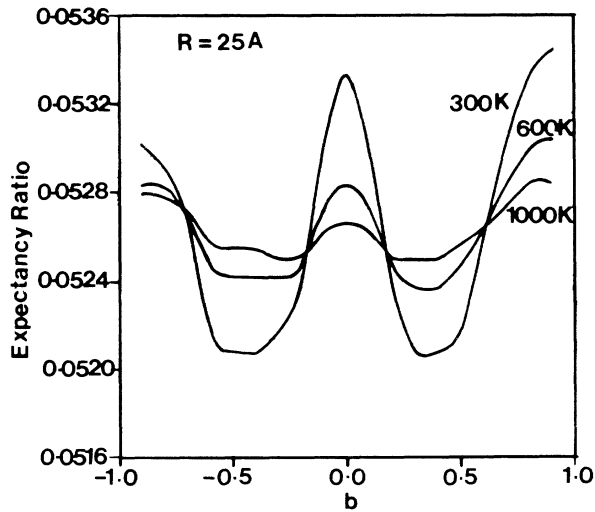


FIG. 2. Boltzmann expectancy of particle structures to go with Fig. 1 at different temperatures.

center) and not on the volume. γ_{111} in the above expression is the surface energy per unit area of a (111) facet and V is the total particle volume. The strains were calculated with a disclination model using inhomogeneous isotropic two-dimensional elasticity. The total potential energy then becomes

$$E = \gamma_{111}E_w V^{2/3} + CV(1 - b^2)^2 + DE_w \gamma_{111} V^{2/3}(1 - b^2) + \dots, \quad (2)$$

where $C = \mu \epsilon_D^2 / 4(1 - \nu)$ and $D = 0.5 \epsilon_D \partial \gamma_{111} / \partial e_s$, with μ the shear modulus, $\epsilon_D = \omega / 2\pi$, ω the disclination angle,⁷ ν Poisson's ratio, and e_s the surface strain. The first three terms in the above expression correspond to contributions due to surface free energy, internal elastic strain energy, and energy from surface distortion. Higher-order terms due to thermal gradients, surface relaxations, etc., were found to be negligible in comparison. To convert this to a Gibbs free energy, one has to take account of the entropy of the anisotropic nature of surface free energy,⁸ the entropy of the total strain energy via the temperature dependence of the elastic moduli,⁹ and the entropy due to dilatation.⁹ The entropy contribution was evaluated as

$$S = E_w \gamma_s V^{2/3} + CV \mu_T (1 - b^2)^2 - 3\beta dV k, \quad (3)$$

where $\gamma_s = d\gamma_{111} / dT$, $\mu_T = d\mu / dT$, β is the Grüneisen constant, dV is the net dilatation in atomic volumes, and k is Boltzmann's constant. In principle one should include the entropy due to surface stresses and that of the twin boundaries in the multiply twinned particles, but analysis indicated that these were negligible. The entropy of mixing was the same for all the shapes as the degeneracies are identical. It should also be noted that a number of terms will not vary with particle structure

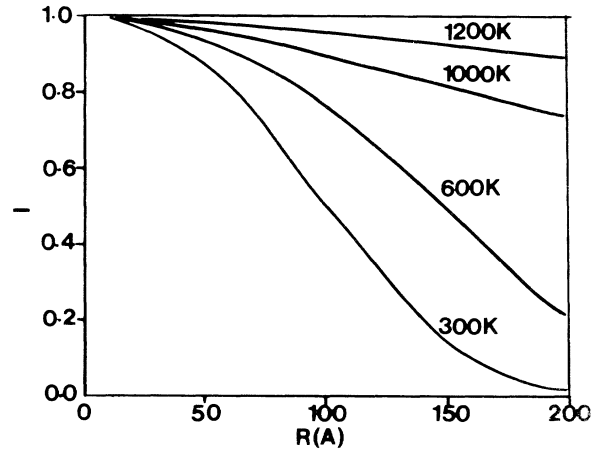


FIG. 3. The index of quasimelting (I), shown as a function of particle radius and temperature. True quasimelting is defined at an arbitrary value of $I = 0.98$.

beyond what we have already considered, for instance, the surface phonon contribution. A typical result for the Gibbs free energy is shown in Fig. 1, here for a 2.5-nm-radius particle.

From these data we can immediately calculate the Boltzmann distribution of particle morphologies as a function of temperature, as shown in Fig. 2. It is clear that these data and the free-energy curves that at higher temperatures there is no preferred structure, and quasimelting will occur. In order to quantify when quasimelting does take place we have chosen to consider an index

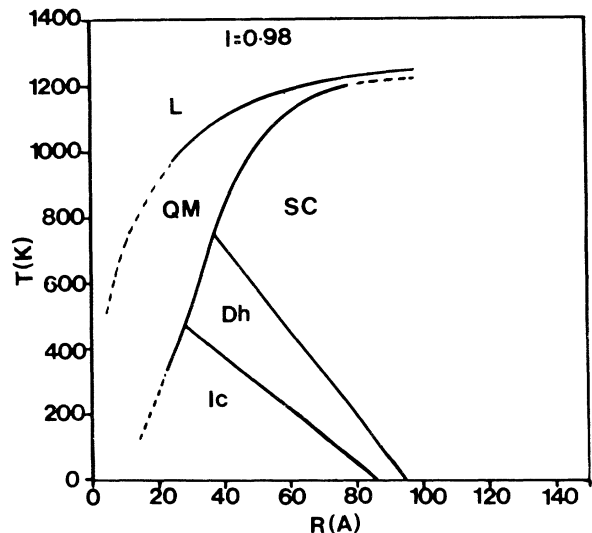


FIG. 4. Phase diagram for small particles. Included in the figure is the experimentally determined depression of the melting point in small particles (Ref. 10). Stability regimes: L, liquidus; QM, quasimelt; Ic, icosahedral multiply twinned particle; Dh, decahedral multiply twinned particle; and SC, single crystal. The phase boundaries shown by dotted lines are extrapolated.

of quasimelting (J), the ratio of the Boltzmann factor for the most unlikely structure to that for the most likely structure, and plotted this for different radii in Fig. 3. When this ratio is greater than 0.98, we will consider that true quasimelting has occurred. Admittedly this value is a little arbitrary, but it should be fairly representative.

With all this information (the free-energy curves for a range of temperatures and particle sizes, and Fig. 3), we can now construct a true phase diagram for particles as a function of size and temperature, as shown in Fig. 4. A number of important phenomena are apparent from the figure. Firstly, the quasimolten phase is clearly distinct from the liquidus and the stable-particle structures. Secondly, multiply twinned particles are clearly low-temperature phenomena. Finally, we can immediately start to understand the critical role of temperature in small-particle growth. For instance, at higher temperatures when the quasimolten and single-crystal phases are contiguous, we would expect to obtain good epitaxial growth for systems such as gold on KCl, which is consistent with experimental results.¹¹

A final point should be made with respect to Fig. 4: The phase boundaries shown should be semiquantitatively correct but need to be tested by experimental results and perhaps more accurate calculations. When calculating the total surface energies of the particles we have only considered (111) and (100) facets, and if higher-index facets were included the energy barriers between different structures would be a little smaller.⁶ Secondly, in principle pairwise calculations could lead to better theoretical results although it is not clear if these are tractable for large clusters even on supercomputers. Finally, it should be noted that this diagram shows only the thermodynamically lowest-energy configurations, but during particle growth, for instance, kinetic factors will be important. With all these caveats aside, it would seem that the phase-diagram approach is a positive step towards a more fundamental understanding of small-

particle structure and growth.

This work would have been impossible without major contributions at earlier stages of the models by Professor John Dundurs, Professor Archie Howie, and Dr. Elizabeth Yoffe, and was funded by the National Science Foundation through Grant No. DMR 8514779.

¹J. G. Allpress and J. V. Sanders, *Surf. Sci.* **7**, 1 (1967); S. Ino, *J. Phys. Soc. Jpn.* **27**, 941 (1967); T. Hayashi, T. Ohno, Y. Shigeki, and R. Uyeda, *Jpn. J. Appl. Phys.* **16**, 705 (1977).

²L. D. Marks, *Philos. Mag.* **49**, 81 (1984); A. Howie and L. D. Marks, *Philos. Mag.* **49**, 95 (1984).

³J. O. Bovin, R. Wallenberg, and D. J. Smith, *Nature (London)* **317**, 47 (1985); S. Iijima, *J. Electron. Microsc.* **34**, 249 (1985); S. Iijima and T. Ichihashi, *Phys. Rev. Lett.* **56**, 616 (1986).

⁴M. R. Hoare and P. Pal, *J. Cryst. Growth* **17**, 77 (1972).

⁵R. Stephen Berry, Julius Jellenik, and Grigory Natanson, *Phys. Rev.* **30**, 919 (1984).

⁶L. D. Marks, P. M. Ajayan, and J. Dundurs, *Ultramicroscopy* **20**, 78 (1986); J. Dundurs, P. M. Ajayan, and L. D. Marks, *Philos. Mag.* (to be published).

⁷The value of ϵ_D is 0.0205 for a decahedral particle corresponding to a disclination angle ω of 7.5° .

⁸H. O. K. Kirchner and G. A. Chadwick, *Philos. Mag.* **22**, 447 (1970). The value of surface entropy (γ_s) used in the calculation was $1.2 \text{ ergs/cm}^2 \cdot \text{K}$.

⁹H. B. Huntington, G. A. Shirn, and E. S. Wajda, *Phys. Rev.* **99**, 1085 (1955); the value for the change in elastic moduli with temperature $d\mu/dT$ was taken as equal to $-0.38 \times 10^9 \text{ dynes/cm}^2 \cdot \text{K}$ and for the Grüneisen constant, 1.96.

¹⁰P. R. Couchman and C. L. Ryan, *Philos. Mag.* **37**, 369 (1978); M. Hasegawa, K. Hoshino, and M. Watabe, *J. Phys. F* **10**, 619 (1980); J. P. Borel, *Surf. Sci.* **106**, 1 (1980).

¹¹S. Ino, *J. Phys. Soc. Jpn.* **21**, 346 (1966); S. Ino and T. Ogawa, *J. Phys. Soc. Jpn.* **22**, 1369 (1967); K. Heinemann, T. Osaka, H. Poppa, and M. Avalos-Borja, *J. Catal.* **83**, 61 (1983).